[Frontiers in Bioscience 17, 2295-2305, June 1, 2012]

PDCD10 interacts with STK25 to accelerate cell apoptosis under oxidative stress

Heyu Zhang[1,3,4], Xi Ma[5], Xuan Deng[1,3], Yiyu Chen[1,3], Xiaoning Mo[3],Yingmei Zhang[1,3], Hongshan Zhao[2,3], Dalong Ma[1,3]

[1]Department of Immunology, School of Basic Medical Sciences, Peking University, No. 38 Xueyuan Road, Beijing 100191, PR China, [2]Department of Medical Genetics, School of Basic Medical Sciences, Peking University, No. 38 Xueyuan Road, Beijing 100191, PR China, [3]Human Disease Genomics Center, Peking University No. 38 Xueyuan Road, Beijing 100191, PR China, [4]Central Laboratory, Peking University School and Hospital of Stomatology, No. 22 Zhongguancun Nandajie, Beijing 100081, PR China, [5]State Key Lab of Animal Nutrition, China Agricultural University, No. 2 Yuanmingyuan West Road, Beijing 100193, PR China

TABLE OF CONTENTS

1. ABSTRACT

An apoptosis-related protein, cerebral cavernous malformation 3 (CCM3 or PDCD10), has recently been implicated in mutations associated with cerebral cavernous malformation. Herein, we show that PDCD10 interacts with serine/threonine kinase 25 (STK25), an oxidant stress response kinase related to sterile-20 (Ste20) that is activated by oxidative stress and induces apoptotic cell death. Functional investigations indicate that PDCD10 and STK25 protein are up-regulated by H_2O_2 stimulation, and that co-expression of the proteins accelerates cell apoptosis. The induction of small interfering PDCD10 (siPDCD10) or siSTK25 results in decreased endogenous PDCD10 and STK25 expression, which is accompanied by attenuated cell apoptosis. Interaction between PDCD10 and STK25 modulates ERK activity under oxidative stress. PDCD10 stabilizes STK25 protein through a proteasome-dependent pathway. Our findings suggest that PDCD10 might be a regulatory adaptor required for STK25 functions, which differ distinctly depending on the redox status of the cells that may be potentially related to tumor progression.

2. INTRODUCTION

Oxidative stress has been suggested as the common mechanism involved in the development of age-dependent diseases such as cancer, arteriosclerosis, arthritis, neurodegenerative disorders, and other conditions (1, 2). The cumulative production of reactive oxygen species (ROS), which is typical for many cancer cells, is linked to the altered redox regulation of signaling cascades.

Cerebral cavernous malformation 3 (CCM3 or PDCD10) was initially identified within apoptotic cells in our laboratory by depriving the cells of granulocyte macrophage colony-stimulating factor (GM-CSF) (3). PDCD10 interacts with many different proteins to form multiple signaling complexes, such as CCM1/KRIT1-CCM2/OSM complex (4), STRIPAK complex (5), and VEGFR2 (6). PDCD10 is used for several different functions, such as cell proliferation, apoptosis, Golgi assembly, and cell migration, (7-11) and is involved in different signaling pathways (4, 6, 8, 10-13). Mutations in PDCD10 have been confirmed to be involved in the

cerebral cavernous malformations (CCMs), which collectively are a major cause of cerebral hemorrhage (14, 15).

The germinal center kinase III (GCK-III) protein subfamily includes 3 members in mammals: STK24/MST3, STK25/SOK1, and MST4 (16, 17). Since they share similarity with sterile-20 (Ste20), a budding yeast serine/threonine kinase (STK), they belong to the Ste20 family of proteins (17). The GCK-III kinases are involved in 2 important cellular processes: regulation of cell growth (18-21) and regulation of cell migration (22, 23). Specifically, STK25, also known as Ste-20 oxidant stress response kinase 1 (SOK1), is activated by oxidative stress (24-26). Under oxidative stress, STK25 drives the apoptotic response to reactive oxygen species (ROS) and chemical anoxia, dissociates from the Golgi, and translocates to the nucleus (20). These STK25 activities are not involved in known mitogen-activated protein kinase (MAPK) pathways(26, 27).

PDCD10 has been shown to associate with GCK-III kinases (4, 5, 7, 8, 28). Our previous studies have shown that PDCD10 interaction with mammalian sterile twenty 4 (MST4) promotes cell growth and transformation via the modulation of the extracellular signal-regulated kinase (ERK) pathway (8). PDCD10 can also be phosphorylated by STK25 *in vitro* (4). Depletion of PDCD10 or dissociation of PDCD10 from the GM130-GCK-III complex destabilizes GCK-III proteins (7).

In this study, we showed for the first time that PDCD10 and STK25 levels are up-regulated by low concentrations of hydrogen peroxide (H2O2). PDCD10 accelerates apoptosis induced by STK25 under oxidative stress and stabilizes the STK25 protein through a proteasome-dependent pathway. Our findings on the roles of ROS in inducing PDCD10 and STK25 protein expression provide a possibility for antioxidant therapies of clinical human cancers.

3. MATERIALS AND METHODS

3.1. Plasmids, siRNA, and antibodies

The pCDEF-PDCD10 plasmid has been described previously (8). DsRed-Golgi was obtained from Clontech Laboratories Inc.. All other plasmids were constructed using standard molecular biology techniques. All siRNAs, including PDCD10, STK25, and control siRNA, were synthesized by GenePharma Corporation. The sequences of siRNAs against PDCD10 and non-silencing siRNA have been reported previously (8). Specific siRNAs against STK25 with targeting sequence 5¢-GCAUCGAUAACCACACAAA-3¢ and 5¢-ACUUUGGCUCCUACCUAAA-3¢ were designed. The anti-STK25 was from Abnova. The goat polyclonal anti-PDCD10 was from Santa Cruz Biotechnology (Santa Cruz). The anti-caspase 3, anti-cleaved caspase 3, and anti-poly (ADP ribose) polymerase (PARP) antibodies were from Cell Signaling Technology. Polyclonal antibodys against ERK and phosphorylated-ERK were obtained from KangChen Bio-tech. The mouse monoclonal anti-PDCD10 has been described previously (8). IRDye 800-conjugated secondary antibodies against mouse, rabbit and goat IgG were purchased from Li-Cor Bioscience. The fluorescein isothiocyanate (FITC)-conjugated rabbit anti-goat IgG was from Zhongshan Corporation (Beijing, China). The tetramethylrhodamine isothiocyanate (TRITC)-conjugated donkey anti-mouse IgG was from Jackson ImmunoResearch.

3.2. Cell culture, transfection, and treatment

HEK 293, HeLa and COS-7 cells were maintained in Dulbecco's modified Eagle's medium (DMEM) (Invitrogen) supplemented with 10% fetal bovine serum (FBS) and 2 mM L-glutamine. PC-3 cells were cultured in RMPI-1640 (Invitrogen) supplemented with 10% FBS and 2 mM L-glutamine. All cells were maintained at 37°C in a humidified atmosphere with 5% CO2. HeLa, COS-7, and PC-3 cells were transfected by electroporation, as described previously (29). H2O2, ebselen (2-phenyl-1, 2-benzisoselena-zol-3[2H]-one), actinomycin D, ALLN (N-acetyl-Leu-Leu-norleucine), and cycloheximide were obtained from Sigma (St. Louis, MO) and freshly reconstituted with dimethylsulfoxide (DMSO) before use.

3.3. Yeast two-hybrid screening

The two-hybrid screening system was used as previously described (Ito *et al.*,2000). Briefly, the library consisted of 1500 known genes associated with cell apoptosis, cell proliferation, and cell cycles. Each open reading frame (ORF) was amplified by polymerase chain reaction (PCR) using Pfu DNA polymerase and cloned into pGBK-RC, a Gal4 DNA-binding domain-based bait vector, and pGAD-RC, a Gal4 activation domain-based prey vector, according to the MATCHMAKER GAL4 Two-Hybrid System 3 and Libraries User Manual PT3247-1 (PR94575) protocol (Clontech). Plasmids with inserts of expected sizes were confirmed by colony PCR and agarose gel electrophoresis. The PDCD10 bait vector and prey vectors were cotransfected in yeast Y190 and plated on synthetic defined medium lacking Leu, Trp, and His (SD/-T-L-H). Well-formed colonies were selected and removed, cracked in liquefacient nitrogen, and subsequently utilized in colony lift filter assays.

3.4. RNA isolation, reverse transcriptase-polymerase chain reaction, and quantitative real-time PCR analysis

RNA was extracted from the cells using TRIzol reagent (Invitrogen) and was reverse transcribed with the ThermoSCRIPT reverse transcriptase-polymerase chain reaction (RT-PCR) System (Invitrogen), according to the manufacturer's protocol. PCR amplification primers and conditions were as follows. PDCD10 forward primer: 5¢-ATGAGGATGACAATGGAAGAGATG-3¢, reverse primer: 5¢-TCAGGCCACAGTTTTGAAGGT-3¢, cycling conditions: 30 cycles (30 s at 94°C, 60 s at 55°C, and 30 s at 72°C); STK25 forward primer: 5¢-ATGGCTCACCTCCGGGGATTTG-3¢; reverse primer: 5¢-TCAGCGGGTGGATGTCAGGTGG-3¢, and the PCR reaction was performed at an annealing temperature of 58°C for 30 cycles. PDCD10 real-time PCR primers were forward: 5¢-AGACACTGAGAGCCGCTTTCA-3¢ and

reverse: 5¢-CCATACGAAGAAGGACTCCG-3¢. STK25 real-time PCR primers were forward: 5¢-TATCTGCACTCCGAACGCAA-3¢ and reverse: 5¢-TCTGCGTGTCTGTGAGCTGC-3¢. Glyceraldehyde-3-phosphate dehydrogenase (GAPDH) was amplified as an internal control. PCR products were separated by electrophoresis on a 1.0% agarose gel and visualized by staining with ethidium bromide.

3.5. Immunoprecipitation and western blot

Cells were collected for the immunoprecipitation (IP) experiment and resuspended in lysis buffer [300 mM sodium chloride (NaCl); 50 mM Tris, pH 8.0; 0.4% nonidet P40 (NP-40); 10 mM magnesium chloride (MgCl2); and 2.5 mM calcium chloride (CaCl2)] supplemented with protease inhibitors (Complete mini EDTA-free; Roche Diagnostics, Mannheim). After centrifugation, the protein in the supernatant were quantified using the bicinchoninic acid (BCA) protein assay reagent (Pierce). Next, 1 mg total cell extract was diluted to 1 ml in dilution buffer (50 mM Tris, pH 8.0; 0.4% NP-40). Following precleaning with protein G sepharose beads, cell lysates were incubated with appropriate antibodies overnight at 4°C, followed by incubation with 50 µl of 50% protein G sepharose slurry for 2 hours. The resulting immunoprecipitates were washed 5 times in washing buffer (50 mM Tris, pH 8.0; 150 mM NaCl; 0.4% NP-40; and 5 mM MgCl2) and analyzed by Western Blot, as described previously (29). An IRDye 800CW-conjugated secondary antibody was used to visualize the proteins; the infrared fluorescent images were obtained using an Odyssey infrared imaging system (Li-Cor Bioscience).

3.6. Immunofluorescence analysis

Cells were transiently transfected with both pEGFP-C3-PDCD10 and pDsred-N1-STK25 plasmids and then plated on glass coverslips. After 24 hours, the cells were fixed [30 min, room temperature, 4% paraformaldehyde (PFA) (wt/vol)], quenched (10 min, 50 mM ammonium chloride), and permeabilized [5 min, 0.1% Triton X-100 (vol/vol)]. The cellular nucleus was stained with 4′-6-diamidino-2-phenylindole (DAPI) (1:10000) for 5 min. Samples were observed using an Olympus Fluoview FV300 laser-scanning confocal microscope (Olympus).

For the endogenous immunefluorescence microscopy of PDCD10 and STK25, the HeLa cells were plated on glass coverslips, cultured for 24 h, fixed, quenched, and permeabilized, as described above. Next, the cells were incubated with anti-PDCD10 and anti-STK25 antibodies and visualized by incubation with FITC-conjugated rabbit anti-goat IgG and TRITC-conjugated bovine anti-mouse IgG, respectively. Subsequently, the coverslips were handled, and the cells were detected in the same manner.

3.7. Cell apoptosis assay

The treated cells (5 × 105) were trypsinized, washed twice with phosphate buffered saline (PBS), and resuspended in 200 µl binding buffer (10 mM HEPES, pH7.4; 140 mM NaCl; 1 mM MgCl2; 5 mM KCl; and 2.5 mM CaCl2). FITC-conjugated Annexin V was added to a final concentration of 0.5 µg/ml, according to the manufacturer's instructions (Biosea), and incubated for 20 min at room temperature in the dark. After washing two times, the samples were immediately analyzed on a FACSCalibur flow cytometer (Becton Dickinson, San Jose, CA).

3.8. Statistical analyses

The results are expressed as the mean±SD. Statistical analysis was performed by the Student's t-test using SPSS13.0 software. All tests were two-sided, and $P < 0.05$ was considered significant.

4. RESULTS

4.1. PDCD10 interacts with STK25 and co-localizes with STK25

Since it did not demonstrate autonomous transactivation and promoter binding activity, PDCD10 was used as bait for Y2H analysis. The PDCD10 transforming efficiency in the Y2H screening reached 4 × 103 colonies/µg of library plasmids, which meets the requirement for library screening. Plasmids from positive yeast colonies were extracted and transformed into Escherichia coli. The prey fished by PDCD10 contained STK25 library plasmids. To exclude false-positive results, we retested the interaction by simultaneously transforming Y190 with the bait (PDCD10) and the prey (STK25) plasmids; for negative controls, pGBT9 vector + STK25 and pGBT7-Lam + STK25 were used. PDCD10 interacted with STK25 in yeast cells. Data from colony lift filter assays confirmed that PDCD10 was able to bind to STK25 in yeast cells (data not shown).

To confirm the association of PDCD10 and STK25 in mammalian cells,Flag-PDCD10 and myc-STK25 plasmids were cotransfected into 293T cells. The immunoprecipitation results showed that myc-STK25 pulled down flag-PDCD10, whereas the empty flag control plasmid did not, suggesting that PDCD10 was able to bind to STK25 in mammalian cells (Figure 1A). Endogenous coimmunoprecipitation analysis further provided evidences for the endogenous PDCD10-STK25 interaction (Figure 1B and C).

To further confirm the PDCD10-STK25 association, we performed a colocalization assay. We constructed fluorescent plasmids pEGFP-C3-PDCD10 and pDsred-N1-STK25 and cotransfected HeLa cells with them. Cell nucleus morphology was observed by DAPI staining. As shown in Figure1D, either pEGFP-C3-PDCD10 or pDsred-N1-STK25 localized to the cytoplasm with some highly concentrated spots around the nucleus, and the distribution of PDCD10 entirely overlapped with STK25. Figure 1E showed that PDCD10 was located in the cytoplasm and was concentrated in areas near the nucleus, overlapping with Golgi. We also investigated the endogenous subcellular locations of PDCD10 and STK25 and found that PDCD10 distribution overlapped with STK25 (Figure 1F).

4.2. PDCD10 and STK25 proteins are up-regulated under oxidative stress conditions and mediated by ROS

We used RT-PCR and Western Blot to confirm differential mRNA and protein expression levels of PDCD10 and STK25 respectively,. As shown in Figure 2A,

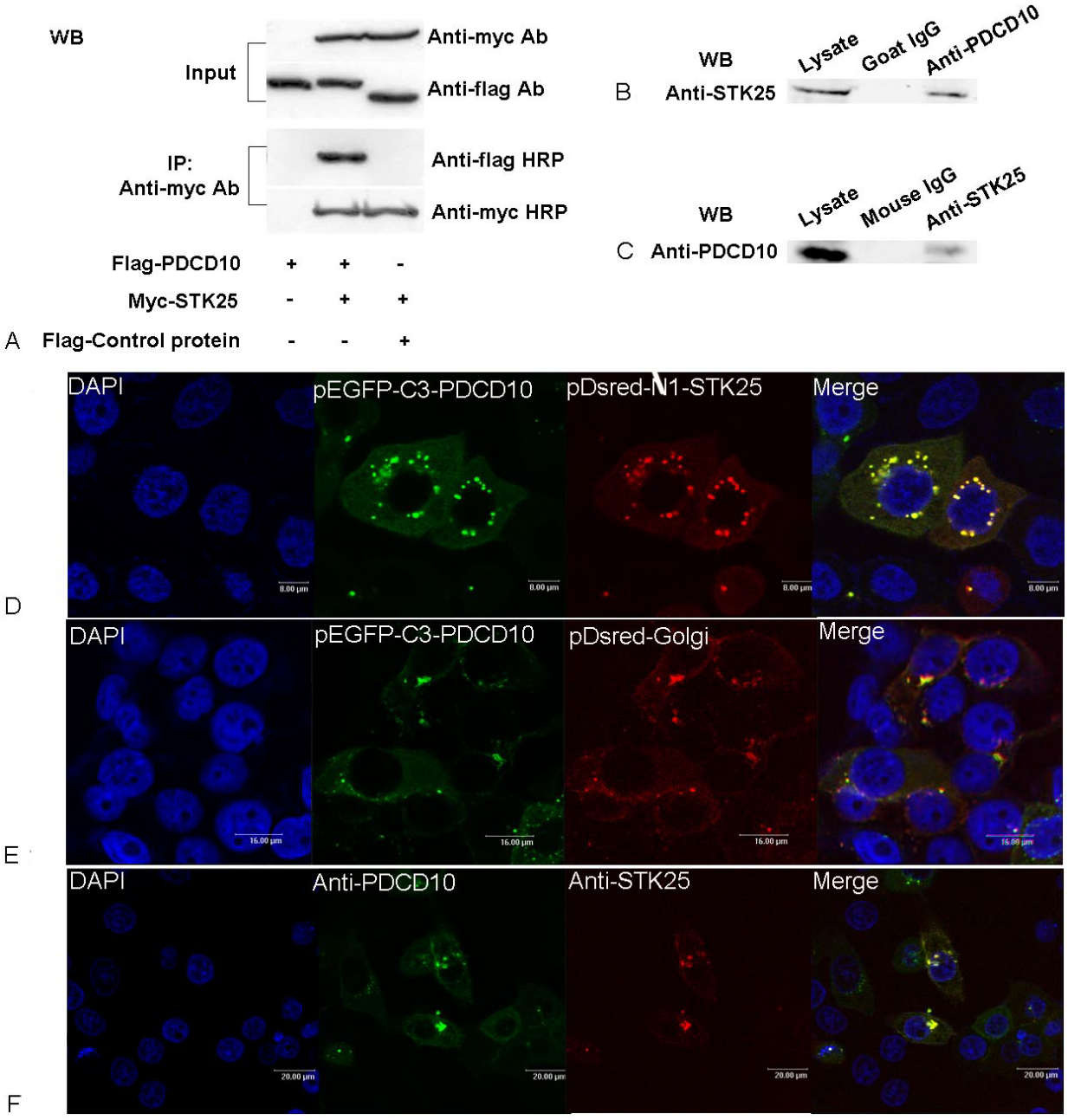

Figure 1. PDCD10 interacted and collocated with STK25. (A) Cell lysates transfected with the indicated constructs were immunoprecipitated with the anti-flag antibody to precipitate Flag-PDCD10 and Flag control protein. Immunoprecipitated proteins were analyzed for the presence of STK25 by Western Blot. (B) Total cell extracts were subjected to IP using either an anti-PDCD10 or an irrelevant control IgG, as indicated. Immunoprecipitated proteins were then analyzed for the presence of STK25 by Western Blot. (C) As in (B),except that cell extracts were immunoprecipitated with an anti-STK25 antibody and immunoblotted with an anti-PDCD10 antibody. (D) Confocal microscopy images of HeLa cells cotransfected with pEGFP-C3-PDCD10 (green) and pDsred-N1-STK25 (red) plasmids, with Coexpression in yellow. Cell nuclei were stained by DAPI staining (blue). (E) pEGFP-C3-PDCD10 (green) and pDsred-N1-Golgi (red) were transfected into HeLa cells together. Images were captured after 36 hours of transfection. (F) The HeLa cells were costained by anti-PDCD10 antibody and FITC-conjugated rabbit anti-goat IgG, anti-STK25 antibody, and TRITC-conjugated donkey anti-mouse IgG, for the endogenous immunofluorescence microscopy of PDCD10 and STK25. It exhibited that either PDCD10 or STK25 localized around the nucleus as highly concentrated spots, and the distribution of PDCD10 overlapped with STK25. Experiments were performed in triplicate with similar results.

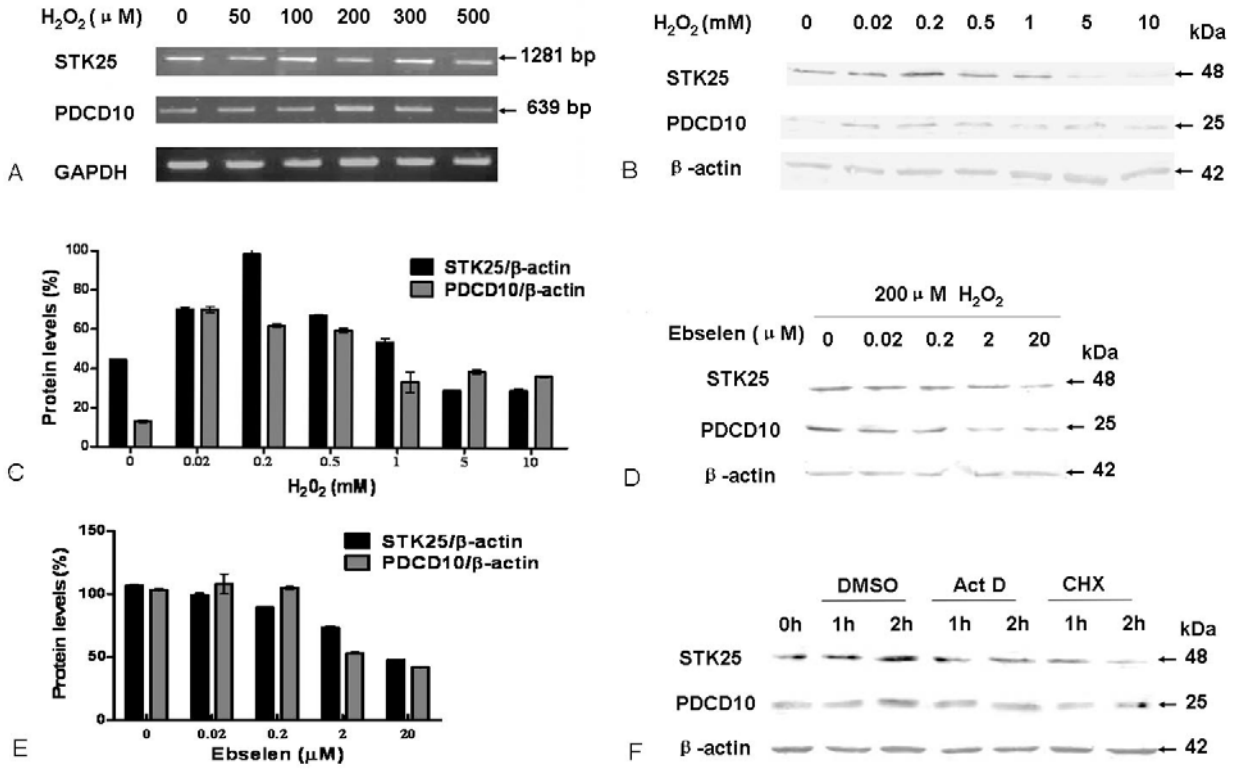

Figure 2. The induction of PDCD10 and STK25 expression by H2O2. (A) HeLa cells were exposed to different concentrations of H2O2 for 24h and then harvested and analyzed by RT-PCR. GAPDH was used as a control. (B) Western Blot analysis of STK25 and PDCD10 in HeLa cells exposed to different concentrations of H2O2 for 4 h. (C) Relative STK25 and PDCD10 protein levels in (B) were quantified using a Li-Cor Odyssey scanner. This experiment has been performed three times. This diagram presented is the statistical analysis of a single representative experiment. (D) Antioxidant ebselen blocked H2O2-induced STK25 and PDCD10 expression in a concentration-dependent manner of HeLa cells. HeLa cells were cultured in the presence of 200 μmol/L H2O2 for 2 hours and in the presence of ebselen (0.02-20 μmol/L) for an additional 2 hours. (E) Relative STK25 and PDCD10 protein levels in (D) were quantified using a Li-Cor Odyssey scanner. (F) Effects of antinomycin D (Act D) and cycloheximide (CHX) on STK25 and PDCD10 protein expression up-regulated by hydrogen peroxide. HeLa cells were exposed to hydrogen peroxide (200 umol/L) for 2 hours and then exposed to 1μg/mL actinomycin D or 100ug/mL cycloheximide or vehicle (DMSO) for 1 and 2 hours. Total cell lysates were analyzed for the presence of STK25 and PDCD10 by Western Blot.

no significant change in the levels of either STK25 or PDCD10 mRNA resulted when cells were exposed to different H2O2 concentrations.

Following 4 hours of stimulation with H2O2 at 0.02–10 mM, STK25 protein expression was observed to increase by 1.2–2-fold over the baseline levels when the H2O2 concentrations were less than 1 mM and PDCD10 expression increased by 2.8–7-fold (Figure 2B and C). STK25 protein expression was down-regulated by high concentrations of H2O2 (>1 mM).

To confirm specific protein regulation by H2O2, we treated cells with ebselen, a scavenger of H2O2 and hydroperoxides. The induction of both PDCD10 and STK25 protein expression in HeLa cells by H2O2 can be effectively antagonized by ebselen in a concentration-dependent manner with an effective blockade at 2 uM ebselen (Figure 2D and E).

STK25 and PDCD10 protein expression up-regulation by H2O2 requires active gene transcription and translation. To determine if the up-regulation of both STK25 and PDCD10 proteins by H2O2 requires active mRNA and protein synthesis, we monitored the steady state of STK25 and PDCD10 protein expression after exposing cells to actinomycin D (inhibitor of RNA synthesis) or to cycloheximide (inhibitor of protein synthesis). Fig2F showed that induction of both STK25 and PDCD10 protein expression in HeLa cells by H2O2 was rapid in onset and could be blocked within 1–2 hours by the addition of cycloheximide to the cell culture medium. However, we found that this short-term (1–2 hours) exposure to actinomycin D slightly altered the accumulation of the two proteins.

4.3. Coexpression of PDCD10 and STK25 accelerates H2O2-induced apoptosis and modulates ERK kinases activity

To investigate the functional significance of STK25 targeting by PDCD10, a series of experiments were conducted. HeLa, COS-7, and PC-3 cells were transfected as indicated, and apoptosis was induced by H2O2. Either

PDCD10 or STK25 alone could effectively promote HeLa cell apoptosis compared to controls upon exposure to H2O2 (Figure 3A and B). Overexpression of both PDCD10 and STK25 produced a synergistic effect indicated by the increase in Annexin V-positive cells, along with the increase in Caspase 3 cleavage (Figure 3C) and PARP cleavage (Figure 3D). Moreover, knockdown of endogenous PDCD10 inhibited STK25-dependent cell apoptosis, as indicated by the decrease in apoptotic cells (Figure 3E and F) and reduced PARP cleavage (Figure 3G left panel). Conversely, we also observed that knockdown of STK25 impaired the apoptotic cell response mediated by PDCD10 overexpression, indicating that the apoptosis-promoting effect of PDCD10 was, at least in part, STK25-dependent (Figure 3G right panel).

H2O2 has been reported to activate MAPK, including the ERK, JNK and p38 pathways. PDCD10 is involved in MAPK signaling pathways (8, 10, 30). We investigated the response of these canonical pathways to ROS signaling. As expected, all three MAPKs were phosphorylated upon H2O2 treatment (Figure 3H and I; results not shown for JNK and p38). Overexpressed PDCD10 or STK25 increased ERK activity at similar levels. Cooverexpressed both PDCD10 and STK25 resulted in a synergistic effect significantly (Figure 3H). In contrast, knockdown of both PDCD10 and STK25 with siRNAs decreased ERK activity (Figure 3I). PDCD10 and STK25 were not involved JNK and p38 pathways under oxidative stress (data not shown).

4.4. PDCD10 enhances the stability of STK25 protein

To assess the role of the PDCD10-STK25 association, we monitored the changes of STK25 levels in conditions of PDCD10 over-expression or depletion. HeLa cells were cotransfected for 24 and 48 hours with either PDCD10 or specific siRNAs against PDCD10. Western Blot analysis indicated a strong increase in STK25 protein levels in cells overexpressing PDCD10 compared to cells transfected with an empty vector (Figure 4A). Meanwhile, STK25 protein levels decreased dramatically after knockdown of endogenous PDCD10 (Figure 4B). We also detected a weak reduction in PDCD10 protein expression when endogenous STK25 was knocked down after 36 and 48 hours (Figure 4C). We further examined the mRNA levels of STK25 after treatment with siRNAs against PDCD10. HeLa cells were transfected for 24, 36, and 48 hours with either siPDCD10 or control siRNA, and cells were then harvested and analyzed by real-time PCR. As shown in Figure 4D, knockdown of PDCD10 failed to influence the STK25 mRNA levels, indicating a potential absence of PDCD10 regulation of STK25 at a transcriptional level.

We next tested the influence of PDCD10 on the half-life of STK25. HeLa cells were transiently transfected with either PDCD10 or siRNA against PDCD10. Cells were then treated with the translation inhibitor CHX (100 μg/ml) for different periods as indicated. As shown in Figure 4E, overexpression of PDCD10 prolonged the half-life of STK25. Because STK25 protein levels were very low when PDCD10 was knocked down, we stimulated the cells with 200 μM H2O2. After 4 hours of H2O2 exposure, the depletion of endogenous PDCD10 was found to be associated with a significant acceleration in STK25 decay, which suggested that the decrease of STK25 protein levels following PDCD10 knockdown was due to the destabilization of the PDCD10 proteins (Figure 4F and G).

After treatment with the ALLN at 100 μM for 6 hours, the STK25 reduction induced by PDCD10 knockdown was significantly blocked (Figure 4H). This suggested that the proteasome inhibitor (ALLN) could rescue siPDCD10-mediated degradation of STK25, indicating that endogenous PDCD10 may be involved in the modulation of STK25 levels in normal growing cells by protecting STK25 from proteasomal degradation.

5. DISCUSSION

The biological and physiological functions of the interaction between PDCD10 and STK25 are the subject of debate. First, we confirmed the interaction between PDCD10 and STK25 by different methods, which agreed with previous studies (4, 7, 21). Our previous research showed that PDCD10 functioned as a positive regulator of MST4 to promote cancer cell growth (8). Therefore, we had hypothesized that PDCD10 may inhibit cell apoptosis that is induced by STK25 under oxidative stress. However, the data of the present study showed that PDCD10 exerted the opposite effect. Similar findings were obtained in COS-7, HeLa, and PC-3 cells, regardless of the endogenous PDCD10 level of expression, which suggested that the biological effects of PDCD10 were not cell-type specific.PDCD10 can be phosphorylated by STK25 *in vitro* (4, 28). We think PDCD10 may function as a substrate of STK25 *in vivo* by exerting a positive feedback regulatory effect on STK25 stability.

The GCK-III subfamily regulates diverse cellular events, including cellular apoptosis, proliferation, and motility (23). The activation of both STK25 and STK24 has been reported to be stimulated by ROS (20, 31). Although PDCD10 forms a complex with GCK-III proteins, including MST4 and STK25, PDCD10 exerts opposite effects under different conditions. It is also possible that PDCD10 cooperates with a different protein preferentially under various stresses: with MST4 in normal conditions and with STK25 under oxidative stress conditions, similar to AP-1, the outcome of which seems to be dependent on AP-1 dimer composition, as well as on the cellular and genetic contexts (32). The function of PDCD10 depends on the degree of ROS associated with the cancer. Significant new studies will be necessary to evaluate this process and to clarify the pathophysiologic role of PDCD10.

PDCD10 is reportedly up-regulated in some carcinomas (33-35), suggesting its role in tumor signaling. The role of PDCD10 in tumor progression can be elucidated from two perspectives. On one hand, ROS-mediated apoptosis induced by PDCD10 and STK25 may be involved. ROS are known to play a dual role as both a beneficial and deleterious species in biological processes (1, 36). Mounting evidence suggests that increased steady-

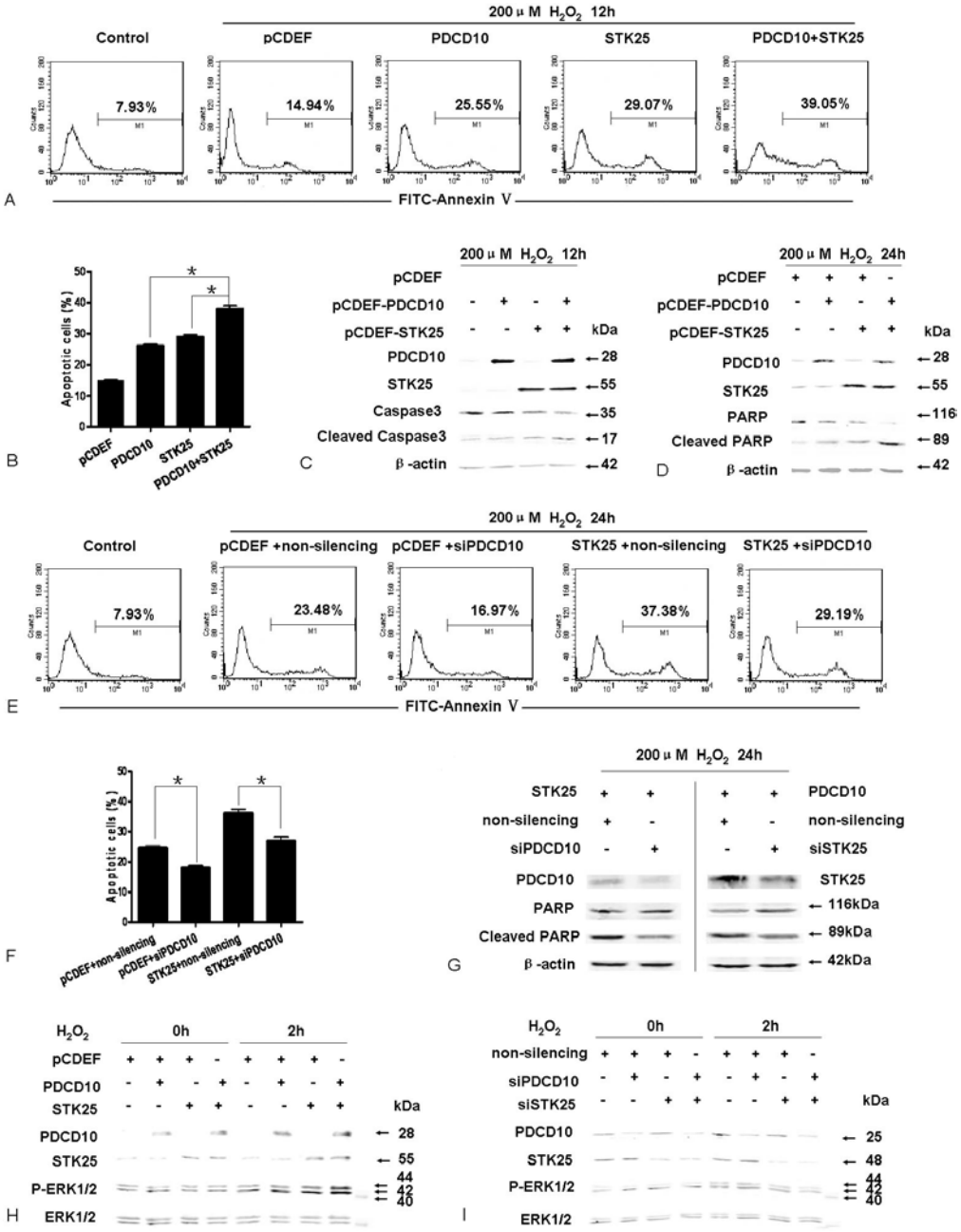

Figure 3. Coexpression of PDCD10 and STK25 accelerates H2O2-induced cell apoptosis. (A) PC-3 cells were transfected with PDCD10 and STK25 plasmids alone or together. After 24 hours, they were exposed to 200μM of H2O2 for 12 hours. Then cells were harvested and stained with annexin V and analyzed by FACS. The data shown are from a representative experiment. (B) Graphic representation of apoptotic cells as a percentage of total cells in three independent experiments as the same in (A). Error bars were calculated as means ± SD. *P<0.01. (C) Caspase-3 cleavage was analyzed by Western Blot. HeLa cells transfected with the indicated plasmids were treated with 200μM of H2O2 for 12 hours and then harvested. (D) HeLa cells transfected with the indicated plasmids were treated with 200μM of H2O2 for 24 hours and PARP cleavage was analyzed. (E) Cells were transfected with the indicated siRNA or plasmids. After 24 hours, they were exposed to 200μM of H2O2 for 24 hours and analyzed by FACS. (F) All data were obtained from three independent experiments described in (e) and presented as means±SD. *P<0.01. (G) As in (E), except that total cell extracts were analyzed by Western Blot for the presence of PRAP. (H) Interaction between PDCD10 and STK25 modulates ERK activity under oxidative stress. Cells transfected with indicated plasmids were subjected to H2O2 (200μM). Cell lysates were separated by SDS-PAGE and immunoblotted with anti-ERK and anti-phospho-ERK. (I) Cells transfected with indicated siRNAs were subjected to H2O2 (200μM).Cells were harvested and separated by SDS-PAGE and probed with respective antibodies.

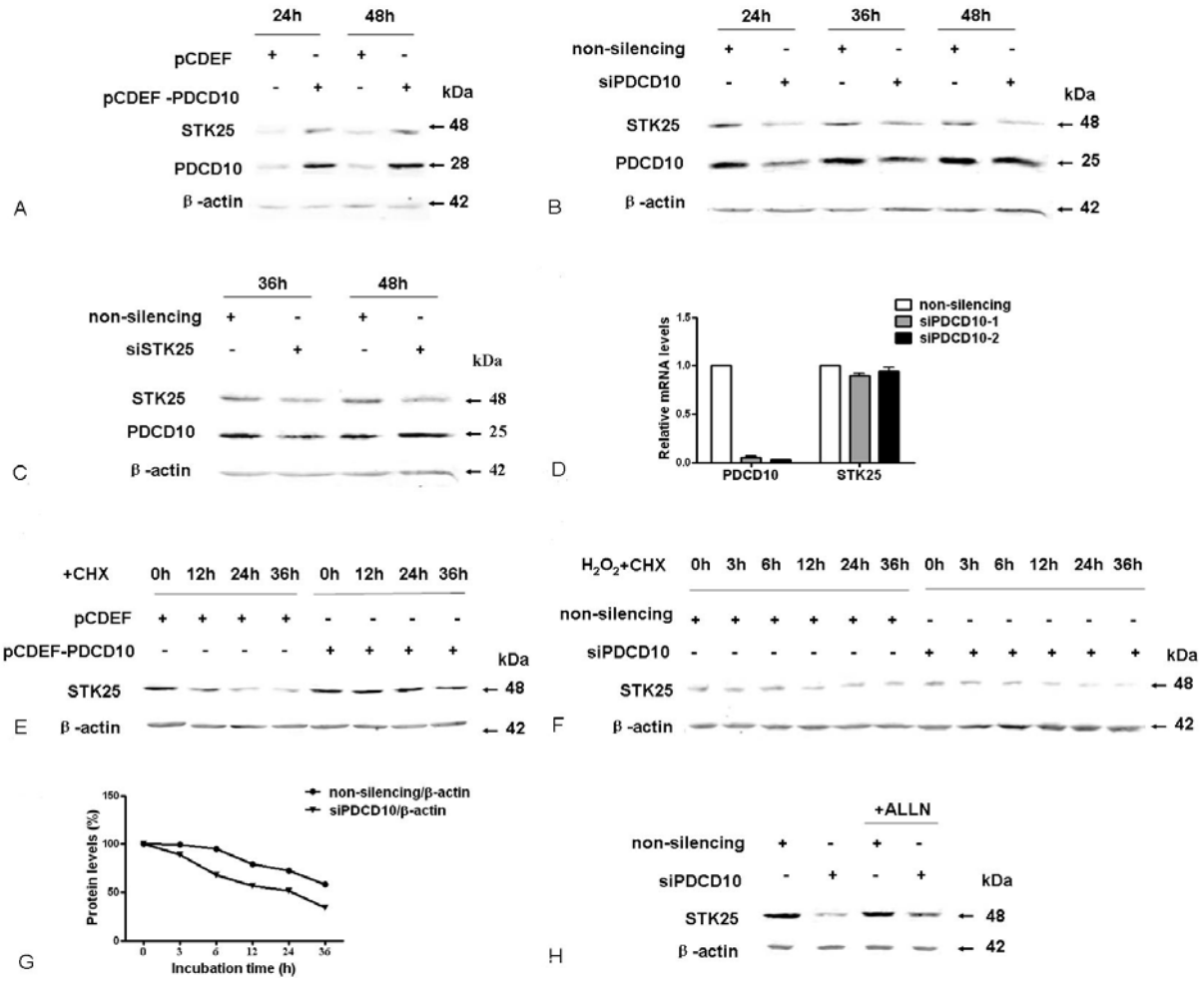

Figure 4. PDCD10 stabilizes STK25. (A) HeLa cells were transfected with the indicated plasmids for 24 or 48 hours. Total cell extracts were analyzed for the presence of STK25 and PDCD10. (B) HeLa cells were transfected with indicated siRNA for 24, 36 and 48 hours and analyzed by Western Blot. (C) HeLa cells were transfected with control siRNA and siSTK25 for 36 and 48 hours and treated as (B). (D) HeLa cells transfected with control siRNA or siPDCD10s for 36 hours were analyzed by real-time PCR. Data were presented as means ± SD. (E) After transfected with indicated plasmids for 24 hours, HeLa cells were treated with 100μg/ml CHX. All cell extracts were prepared at the indicated times and analyzed by Western Blot. (F) HeLa cells were transfected with control siRNA or siPDCD10 for 24 hours. Then cells were exposed to 200μM H2O2 for 4 hours and after that treated by 100μg/ml CHX for different lengths of time as indicated. Total cell lysates were analyzed for the presence of STK25 by Western Blot. (G) The results of relative STK25 protein levels showed in (F) were quantified using a Li-Cor Odyssey scanner. This experiment has been performed three times. This diagram presented is the statistical analysis of a single representative experiment. (H) HeLa cells were transfected with control siRNA or siPDCD10. After 24 hours, cells were treated with ALLN (100 μM) for 6 hours. Total cell lysates were analyzed by Western Blot.

state levels of ROS may trigger transformation and contribute to cancer progression by amplifying genomic instability (37). ROS can also induce cellular senescence and apoptosis and can therefore function as an anti-tumorigenic species (1). Besides, ROS actually enhance cell signaling through many different pathways, such as VEGF signaling pathway (38, 39). Exposure to H2O2 can increase VEGF and VEGFR2 mRNA and protein expression in endothelial cells (38). In response to VEGF stimulation, PDCD10 is recruited to VEGFR2 and stabilize it. which involves Akt, PLC-γ, and ERK pathways (6, 13). During cancer development, this pathway may be activated, and Akt and PLC-γ pathways require more focus. On the other hand, recent evidence indicates that the loss of cell polarity is intimately involved in cancer; several crucial cell-polarity proteins are known to function as proto-oncogenes or tumor suppressors (40). PDCD10 is important for Golgi assembly and for centrosome and Golgi orientation in wound-healing assays (7). Adequate positioning of the centrosome and Golgi has been suggested to reflect a cell's capability to polarize (41). Therefore, PDCD10 may regulate cell migration and polarity, which suggests its important role in cancer development as well, although the *in vivo* mechanism remains to be further elucidated.

CCMs are common vascular malformations characterized by enlarged vessels (caverns) consisting of a single endothelial layer lacking mature vessel wall structure, elastin, and smooth muscle cells (42). Growing evidence suggests that oxidative stress plays an important role in the pathogenesis and development of vascular diseases (43, 44). ROS participate in growth, apoptosis, and migration of vascular smooth muscle cells, in the modulation of endothelial function (including endothelium-dependent relaxation and expression of the proinflammatory phenotype), and in the modification of the extracellular matrix (45). The eNOS-dependent H2O2 generation is associated with late childhood and adult onset of hereditary hemorrhagic telangiectasia disease, which is related to CCM (46). Furthermore, Goitre *et al.* found that CCM1/KRIT1 loss/down-regulation is associated with a significant increase in intracellular ROS (47). ROS may contribute to the pathogenesis of CCM, partly by inducing the apoptosis effect of PDCD10 and STK25, which suggests that the sources of ROS and the signaling pathways involved may be important therapeutic targets.

PDCD10 interacts with multiple complexes, as Dyer *et al* summarized(13). At stoichiometric amounts, PDCD10 interacts with CCM1 and CCM2,the lack of which destabilizes endothelial cell-cell junction by sustaining Rho/ROCK signaling (30). A large portion of PDCD10 binds to GCK-□ kinases and PP2A-striatin-Mob3-STRIP complex . GCK-□ kinases are required for Golgi integrity(7). While STK25 promotes cell migration, MST3 and MST4 kinase activity abolish invasion into collagen via different pathways(23). The caspase-mediated proteolytic activation of MST3 and STK25 contribute cell apoptosis under different stimulations(19, 20). However, MST4 promote cell proliferation(48). Several components of PP2A-striatin-Mob3-STRIP complex are linked to intracellular trafficking in mammalian cells(5). Additionally, PDCD10 also regulates VEGF2R stability and therefore, VEGF signaling pathway which plays an important role of vasculogenesis(6). All these data show that PDCD10 is an important molecular involved in diverse aspects of cell biology and functioned as a regulator of those different proteins. However, the equilibrium between all of these pathways is still unknown and requires an in-depth analysis.

In summary, we showed that the expression of both PDCD10 and STK25 was controlled by ROS and was up-regulated in prostate cancer tissues. Ebselen, a seleno-organic antioxidant, was shown to block PDCD10 and STK25 functions by inhibiting ROS production. PDCD10 functions as an STK25 coactivator to promote cell apoptosis under oxidative stress. An enhanced understanding of the downstream pathways that link PDCD10 to tumorigenesis could potentially be the basis for new clinical cancer therapeutic developments.

6. ACKNOWLEDGEMENTS

This work was supported by grants from the National Natural Science Foundation of China (30872940) and the National Key New Drug Creation Program of China (2009ZX09503-004).

7. REFERENCES

1. M. Valko, C. J. Rhodes, J. Moncol, M. Izakovic and M. Mazur: Free radicals, metals and antioxidants in oxidative stress-induced cancer. *Chem Biol Interact*, 160(1), 1-40 (2006)

2. B. F. Oliveira, J. A. Nogueira-Machado and M. M. Chaves: The role of oxidative stress in the aging process. *ScientificWorldJournal*, 10, 1121-8

3. Y. G. Wang, Liu, H. T., Zhang, Y. M., and Ma, D. L: cDNA cloning and expression of an apoptosis-related gene, human TFAR-15 gene. *Science in China C Life Sci*(29), 331-336 (1999)

4. K. Voss, S. Stahl, E. Schleider, S. Ullrich, J. Nickel, T. D. Mueller and U. Felbor: CCM3 interacts with CCM2 indicating common pathogenesis for cerebral cavernous malformations. *Neurogenetics*, 8(4), 249-56 (2007)

5. M. Goudreault, L. M. D'Ambrosio, M. J. Kean, M. J. Mullin, B. G. Larsen, A. Sanchez, S. Chaudhry, G. I. Chen, F. Sicheri, A. I. Nesvizhskii, R. Aebersold, B. Raught and A. C. Gingras: A PP2A phosphatase high density interaction network identifies a novel striatin-interacting phosphatase and kinase complex linked to the cerebral cavernous malformation 3 (CCM3) protein. *Mol Cell Proteomics*, 8(1), 157-71 (2009)

6. Y. He, H. Zhang, L. Yu, M. Gunel, T. J. Boggon, H. Chen and W. Min: Stabilization of VEGFR2 signaling by cerebral cavernous malformation 3 is critical for vascular development. *Sci Signal*, 3(116), ra26 (2010)

7. M. Fidalgo, M. Fraile, A. Pires, T. Force, C. Pombo and J. Zalvide: CCM3/PDCD10 stabilizes GCKIII proteins to promote Golgi assembly and cell orientation. *J Cell Sci*, 123(Pt 8), 1274-84 (2010)

8. X. Ma, H. Zhao, J. Shan, F. Long, Y. Chen, Y. Chen, Y. Zhang, X. Han and D. Ma: PDCD10 interacts with Ste20-related kinase MST4 to promote cell growth and transformation via modulation of the ERK pathway. *Mol Biol Cell*, 18(6), 1965-78 (2007)

9. E. Schleider, S. Stahl, J. Wustehube, U. Walter, A. Fischer and U. Felbor: Evidence for anti-angiogenic and pro-survival functions of the cerebral cavernous malformation protein 3. *Neurogenetics* (2010)

10. L. Chen, G. Tanriover, H. Yano, R. Friedlander, A. Louvi and M. Gunel: Apoptotic functions of PDCD10/CCM3, the gene mutated in cerebral cavernous malformation 3. *Stroke*, 40(4), 1474-81 (2009)

11. B. Lauenborg, K. Kopp, T. Krejsgaard, K. W. Eriksen, C. Geisler, S. Dabelsteen, R. Gniadecki, Q. Zhang, M. A. Wasik, A. Woetmann and N. Odum: Programmed cell death-10 enhances proliferation and protects malignant T cells from apoptosis. *Apmis*, 118(10), 719-28 (2010)

12. Y. He, H. Zhang, L. Yu, M. Gunel, T. J. Boggon, H. Chen and W. Min: Stabilization of VEGFR2 signaling by cerebral cavernous malformation 3 is critical for vascular development. *Sci Signal*, 3(116), ra26

13. L. A. Dyer, A. L. Portbury and C. Patterson: Gyrate: CCM3 dances with a different angiogenic partner. *Sci Signal*, 3(122), pe17 (2010)

14. B. Guclu, A. K. Ozturk, K. L. Pricola, K. Bilguvar, D. Shin, B. J. O'Roak and M. Gunel: Mutations in apoptosis-related gene, PDCD10, cause cerebral cavernous malformation 3. *Neurosurgery*, 57(5), 1008-13 (2005)

15. F. Bergametti, C. Denier, P. Labauge, M. Arnoult, S. Boetto, M. Clanet, P. Coubes, B. Echenne, R. Ibrahim, B. Irthum, G. Jacquet, M. Lonjon, J. J. Moreau, J. P. Neau, F. Parker, M. Tremoulet and E. Tournier-Lasserve: Mutations within the programmed cell death 10 gene cause cerebral cavernous malformations. *Am J Hum Genet*, 76(1), 42-51 (2005)

16. T. H. Zhou, K. Ling, J. Guo, H. Zhou, Y. L. Wu, Q. Jing, L. Ma and G. Pei: Identification of a human brain-specific isoform of mammalian STE20-like kinase 3 that is regulated by cAMP-dependent protein kinase. *J Biol Chem*, 275(4), 2513-9 (2000)

17. I. Dan, N. M. Watanabe and A. Kusumi: The Ste20 group kinases as regulators of MAP kinase cascades. *Trends Cell Biol*, 11(5), 220-30 (2001)

18. I. Dan, S. E. Ong, N. M. Watanabe, B. Blagoev, M. M. Nielsen, E. Kajikawa, T. Z. Kristiansen, M. Mann and A. Pandey: Cloning of MASK, a novel member of the mammalian germinal center kinase III subfamily, with apoptosis-inducing properties. *J Biol Chem*, 277(8), 5929-39 (2002)

19. C. Y. Huang, Y. M. Wu, C. Y. Hsu, W. S. Lee, M. D. Lai, T. J. Lu, C. L. Huang, T. H. Leu, H. M. Shih, H. I. Fang, D. R. Robinson, H. J. Kung and C. J. Yuan: Caspase activation of mammalian sterile 20-like kinase 3 (Mst3). Nuclear translocation and induction of apoptosis. *J Biol Chem*, 277(37), 34367-74 (2002)

20. E. Nogueira, M. Fidalgo, A. Molnar, J. Kyriakis, T. Force, J. Zalvide and C. M. Pombo: SOK1 translocates from the Golgi to the nucleus upon chemical anoxia and induces apoptotic cell death. *J Biol Chem*, 283(23), 16248-58 (2008)

21. J. Zhou, Z. Shao, R. Kerkela, H. Ichijo, A. J. Muslin, C. Pombo and T. Force: Serine 58 of 14-3-3zeta is a molecular switch regulating ASK1 and oxidant stress-induced cell death. *Mol Cell Biol*, 29(15), 4167-76 (2009)

22. T. J. Lu, W. Y. Lai, C. Y. Huang, W. J. Hsieh, J. S. Yu, Y. J. Hsieh, W. T. Chang, T. H. Leu, W. C. Chang, W. J. Chuang, M. J. Tang, T. Y. Chen, T. L. Lu and M. D. Lai: Inhibition of cell migration by autophosphorylated mammalian sterile 20-like kinase 3 (MST3) involves paxillin and protein-tyrosine phosphatase-PEST. *J Biol Chem*, 281(50), 38405-17 (2006)

23. C. Preisinger, B. Short, V. De Corte, E. Bruyneel, A. Haas, R. Kopajtich, J. Gettemans and F. A. Barr: YSK1 is activated by the Golgi matrix protein GM130 and plays a role in cell migration through its substrate 14-3-3zeta. *J Cell Biol*, 164(7), 1009-20 (2004)

24. C. M. Pombo, T. Tsujita, J. M. Kyriakis, J. V. Bonventre and T. Force: Activation of the Ste20-like oxidant stress response kinase-1 during the initial stages of chemical anoxia-induced necrotic cell death. Requirement for dual inputs of oxidant stress and increased cytosolic [Ca2+]. *J Biol Chem*, 272(46), 29372-9 (1997)

25. K. J. Trouba, K. M. Geisenhoffer and D. R. Germolec: Sodium arsenite-induced stress-related gene expression in normal human epidermal, HaCaT, and HEL30 keratinocytes. *Environ Health Perspec*t, 110 Suppl 5, 761-6 (2002)

26. C. M. Pombo, J. V. Bonventre, A. Molnar, J. Kyriakis and T. Force: Activation of a human Ste20-like kinase by oxidant stress defines a novel stress response pathway. *Embo J*, 15(17), 4537-46 (1996)

27. S. Osada, M. Izawa, R. Saito, K. Mizuno, A. Suzuki, S. Hirai and S. Ohno: YSK1, a novel mammalian protein kinase structurally related to Ste20 and SPS1, but is not involved in the known MAPK pathways. *Oncogene*, 14(17), 2047-57 (1997)

28. K. Voss, S. Stahl, B. M. Hogan, J. Reinders, E. Schleider, S. Schulte-Merker and U. Felbor: Functional analyses of human and zebrafish 18-amino acid in-frame deletion pave the way for domain mapping of the cerebral cavernous malformation 3 protein. *Hum Mutat*, 30(6), 1003-11 (2009)

29. H. Zhang, X. Ma, T. Shi, Q. Song, H. Zhao and D. Ma: NSA2, a novel nucleolus protein regulates cell proliferation and cell cycle. *Biochem Biophys Res Commun*, 391(1), 651-8 (2010)

30. R. A. Stockton, R. Shenkar, I. A. Awad and M. H. Ginsberg: Cerebral cavernous malformations proteins inhibit Rho kinase to stabilize vascular integrity. *J Exp Med,* 207(4), 881-96 (2010)

31. C. B. Chen, J. K. Ng, P. H. Choo, W. Wu and A. G. Porter: Mammalian sterile 20-like kinase 3 (MST3) mediates oxidative-stress-induced cell death by modulating JNK activation. *Biosci Rep*, 29(6), 405-15 (2009)

32. R. Eferl and E. F. Wagner: AP-1: a double-edged sword in tumorigenesis. *Nat Rev Cancer*, 3(11), 859-68 (2003)

33. J. X. Chen, Fan, J. P., Yin, G. K., Sun, A. H., Liao, J. C., Tan, G. R., Huan, G. Y.,Li, Y., Xie, Y., and Mao, Y. M.: Study of differentially expressed genes in laryngeal squamous cell carcinoma by cDNA microarray. *Chin. Acad. J.Sec. Mil. Med. Univ.*(22), 519-522 (2001)

34. S. Huerta, Harris, D. M., Jazirehi, A., Bonavida, B., Elashoff, D., Livingston,E. H., and Heber, D.: Gene expression profile of metastatic colon cancer cells resistant to cisplatin-induced apoptosis. *Int. J. Oncol.* , 22(663-670) (2003)

35. A. J. Aguirre, C. Brennan, G. Bailey, R. Sinha, B. Feng, C. Leo, Y. Zhang, J. Zhang, J. D. Gans, N. Bardeesy, C. Cauwels, C. Cordon-Cardo, M. S. Redston, R. A. DePinho and L. Chin: High-resolution characterization of the pancreatic adenocarcinoma genome. *Proc Natl Acad Sci U S A*, 101(24), 9067-72 (2004)

36. H. Puzanowska-Tarasiewicz, L. Kuzmicka and M. Tarasiewicz: [Influence of reactive nitrogen and oxygen species on human organism]. *Pol Merkur Lekarski*, 27(162), 496-8 (2009)

37. P. T. Schumacker: Reactive oxygen species in cancer cells: live by the sword, die by the sword. *Cancer Cell*, 10(3), 175-6 (2006)

38. F. R. Gonzalez-Pacheco, J. J. Deudero, M. C. Castellanos, M. A. Castilla, M. V. Alvarez-Arroyo, S. Yague and C. Caramelo: Mechanisms of endothelial response to oxidative aggression: protective role of autologous VEGF and induction of VEGFR2 by H2O2. *Am J Physiol Heart Circ Physiol*, 291(3), H1395-401 (2006)

39. M. Ushio-Fukai: Redox signaling in angiogenesis: role of NADPH oxidase. *Cardiovasc Res*, 71(2), 226-35 (2006)

40. M. Lee and V. Vasioukhin: Cell polarity and cancer--cell and tissue polarity as a non-canonical tumor suppressor. *J Cell Sci*, 121(Pt 8), 1141-50 (2008)

41. S. Yadav, S. Puri and A. D. Linstedt: A primary role for Golgi positioning in directed secretion, cell polarity, and wound healing. *Mol Biol Cell*, 20(6), 1728-36 (2009)

42. D. Rothbart, I. A. Awad, J. Lee, J. Kim, R. Harbaugh and G. R. Criscuolo: Expression of angiogenic factors and structural proteins in central nervous system vascular malformations. *Neurosurgery*, 38(5), 915-24; discussion 924-5 (1996)

43. N. Gokce, J. F. Keaney, Jr., L. M. Hunter, M. T. Watkins, J. O. Menzoian and J. A. Vita: Risk stratification for postoperative cardiovascular events via noninvasive assessment of endothelial function: a prospective study. *Circulation*, 105(13), 1567-72 (2002)

44. T. Heitzer, T. Schlinzig, K. Krohn, T. Meinertz and T. Munzel: Endothelial dysfunction, oxidative stress, and risk of cardiovascular events in patients with coronary artery disease. *Circulation*, 104(22), 2673-8 (2001)

45. A. Fortuno, G. San Jose, M. U. Moreno, J. Diez and G. Zalba: Oxidative stress and vascular remodelling. *Exp Physiol*, 90(4), 457-62 (2005)

46. J. Belik, M. Jerkic, B. A. McIntyre, J. Pan, J. Leen, L. X. Yu, R. M. Henkelman, M. Toporsian and M. Letarte: Age-dependent endothelial nitric oxide synthase uncoupling in pulmonary arteries of endoglin heterozygous mice. *Am J Physiol Lung Cell Mol Physiol*, 297(6), L1170-8 (2009)

47. L. Goitre, F. Balzac, S. Degani, P. Degan, S. Marchi, P. Pinton and S. F. Retta: KRIT1 regulates the homeostasis of intracellular reactive oxygen species. *PLoS One*, 5(7), e11786 (2010)

48. J. L. Lin, H. C. Chen, H. I. Fang, D. Robinson, H. J. Kung and H. M. Shih: MST4, a new Ste20-related kinase that mediates cell growth and transformation via modulating ERK pathway. *Oncogene,* 20(45), 6559-69 (2001)

Abbreviations: PDCD10: programmed cell death 10, STK25: serine/threonine kinase 25, H2O2: hydrogen peroxide, DMEM: Dulbecco's modified Eagle's medium, FBS: fetal bovine serum, ALLN: N-acetyl-Leu-Leu-norleucine, CHX: cycloheximide, DMSO: dimethylsulfoxide, PFA: paraformaldehyde, HEPES: 4-(2-hydroxyethyl)-1-piperazineëthanesulfonic acid

Key Wds: PDCD10, STK25, Apoptosis, ERK, Oxidative stress

Send correspondence to: Hongshan Zhao, Department of Medical Genetics , School of Basic Medical Sciences, Peking University, No. 38 Xueyuan Road, Beijing 100191, PR China, Tel: 86-10-82802846-420, Fax: 86-10-82801149, E-mail: hongshan@bjmu.edu.cn